CIRP Annals - Manufacturing Technology 69 (2020) 101–104

Contents lists available at ScienceDirect

CIRP Annals - Manufacturing Technology

journal homepage: https://www.editorialmanager.com/CIRP/default.aspx

Method for determining edge chipping in milling based on tool holder vibration measurements

Friedrich Bleicher (2)[a,*], Christoph Marcus Ramsauer[a], Ralf Oswald[a], Norbert Leder[b], Paul Schoerghofer[a]

[a] IFT - Institute of Production Engineering and Photonic Technologies, TU Wien, Austria
[b] myTool IT GmbH, Austria

ARTICLE INFO

Article history:
Available online 20 May 2020

Keywords:
Milling
Vibration
Modelling
Machine learning

ABSTRACT

Process monitoring and in-process control in milling requires reliable sensor data from rotating tooling systems. Vibration sensing by an instrumented tool holder close to the cutting zone has been proven useful in mitigating chatter. A model is presented that enables the interpretation of vibration data of the rotating sensor and tool system to identify edge chipping. Thus, data from a single axis accelerometer can be interpreted to identify the existence of edge chipping on one of multiple cutting edges. The classification of observed effects is derived from methods developed for machine learning, which is demonstrated and evaluated by experimental results.

1. Introduction

Chipping of cutting edges, especially when machining difficult to machine materials like Inconel 718 [1] or hardened steel [2] with high feed rates, can be caused by poor process conditions and significantly deteriorates the resulting surface quality. Prediction and prevention of chipping is a challenge due to the stochastic characteristics of its initiation and occurrence. Process monitoring using mechatronic systems [3] and sensory machine tool components in various applications enables in-process control (e.g. [4]). Force measurement using piezo-electric components or strain gauges is widely acknowledged to be capable of reliable process monitoring in milling operations [5,6]. In [7], an effort to bring sensors as close as possible to the tool engagement, without being consumable, resulted in the development of an instrumented tool holder with integrated accelerometer. As demonstrated in [8], this relatively low-cost vibration measuring system is used for real-time control to mitigate chatter.

This work describes the development of a process that uses an instrumented tool holder to detect the chipping of cutting edges in end-milling operations. The focus lies not on the event of edge chipping itself and its detection, but on the cutting conditions which reveal just after an event of edge chipping has occurred. In the analysis of respective acceleration signals a mechanical model of the MEMS-sensor is implemented. The data-driven tuning of the resulting algorithm, which is able to determine the occurrence and state of edge chipping, is addressed by the Random Forest Method, a method of machine learning.

2. Test setup

Experimental investigations were performed on a 5-axis CNC milling center (DMG Mori, DMU75 monoBLOCK), using an end mill (Boehlerit, BS90 AP10.016) with a diameter $d = 16$ mm and two cutting inserts. The workpiece material was tool steel 40CrMnMoS8-6 (1.2312), in quenched and tempered condition, with a yield strength of 1100 MPa. During initial cutting tests the resulting forces were measured by a rotating dynamometer (Kistler, 9170A) while milling along a straight path of $L_f = 160$ mm (cutting parameters see Fig. 2). A run-in period was applied to new inserts under constant conditions to generate a basic cutting edge state as reference (27 cycles; $L_f = 4.3$ m; $t = 4.02$ min). In Fig. 1, this reference state is referred to as condition C1.1 or C1.2, respectively. In order to simulate irregular tool wear, as it occurs due to edge chipping, one of the two inserts on

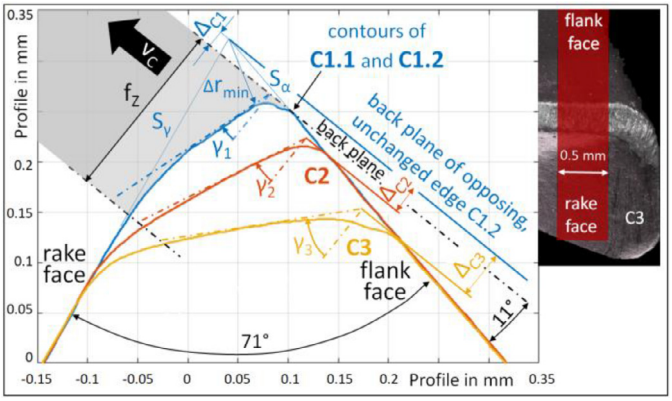

Fig. 1. Tool wear conditions and evaluated section of major cutting edge.

* Corresponding author.
E-mail address: bleicher@ift.at (F. Bleicher).

https://doi.org/10.1016/j.cirp.2020.04.100
0007-8506/

Table 1
Geometric parameters of modified cutting edges.

Condition	Δr_{min} in μm	S_α in μm	S_γ in μm	K	Δ_{Ci} in μm	γ_{eff} in °
C1.1 (reference)	70	92	220	2.39	12	−12
C2 (first wear state)	123	14	262	1.79	24	−25
C3 (second wear state)	184	264	283	1.07	43	−42

the end mill was replaced by artificially worn inserts (Fig. 1: conditions C2 and C3), while the opposing insert was kept at the reference state (C1.2) for all experiments. Fig. 1 depicts these cutting edge conditions.

The artificially worn cutting edges were created with a tool grinding process and post treatment in order to realize a defined and homogenous modification of the cutting edge and corner radius. The shapes of the artificial geometric modifications are realized according to real tool wear geometries, which regularly show for edge chipping highly negative rake angles at form factors $\kappa > 1$ [9]. Optical metrology (Alicona Edge-Master) was used to measure the cutting edges: the mean value was calculated from one thousand profiles within a section of 0.5 mm width (Fig. 1). Table 1 gives an overview of different parameters, which describe the cutting-edge micro geometry of the inserts.

Monitoring the process with a rotational dynamometer (Kistler, 9170A) reveals the prevailing process dynamics when one insert has experienced significantly more wear than the other one (Fig. 2). This experimental procedure replicates the effects of irregular tool wear on the cutting edges, for example as a result of chipping, cratering, and cracking, which may occur spontaneously on one cutting edge. The result of a precipitate wear event on one insert of an end mill is reduced specific feed on the chipped edge, and thus, locally decreased cutting forces. This change in tool geometry causes the other cutting edge to experience an increased feed as compared to nominal conditions. The cutting conditions at the chipped edge generate higher cutting forces due to negative rake angles. In general, both effects co-exist and superimpose.

Wear alters the radial position of the cutting edges. Fig. 3 shows the effect of wear geometry at the cutting insert for end milling and thus the influence on the uncut chip thickness. Hence, the radial alignment and position of the cutting edge is taken into account by the offset of the cutting edge $\pm\Delta_{Ci}$.

$$F_c = k_{c1.1}, \cdot h \cdot a_p \cdot K_h \cdot K_\gamma \tag{1}$$

$$K_h = \frac{k_c}{k_{c1.1}} = \left(\frac{h}{1mm}\right)^{-0.17} \tag{2}$$

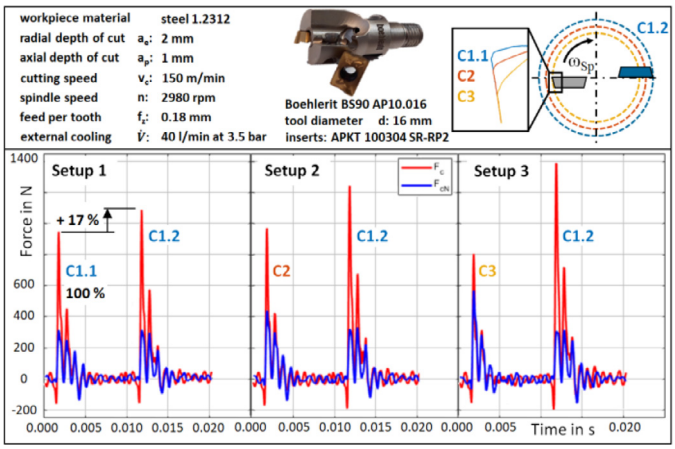

Fig. 2. Cutting force F_c (red) and F_{cN} (blue) measurement for different edge geometry states and resulting radial positions in a highly interruptive cut. (For interpretation of the references to colour in this figure legend, the reader is referred to the web version of this article.)

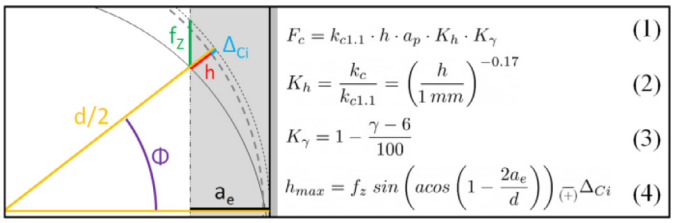

Fig. 3. Geometric relations and mechanistic cutting force model [10].

$$K_\gamma = 1 - \frac{\gamma - 6}{100} \tag{3}$$

$$h_{max} = f_z \sin\left(acos\left(1 - \frac{2ae}{d}\right)\right)_{(\cdot)^{\Delta Ci}} \tag{4}$$

Based on the equation of the mechanistic cutting force model (Eq. (1)), the correction factors of cutting force (Eq. (2) and 3), confirm the effect of tool wear considering both cutting edges. The term $h_{max} \bullet K_\gamma \bullet K_h$ is proportional to the cutting force. Thus, the analytical results in Table 2 refer to C1.1 (100%) and estimate a slight change of the cutting force on the modified edges, but a significant increase on the opposite edge (always condition C1.2) due to the increase in the uncut chip thickness h_{max} (cf. Eq. (4)).

Having quantified the effect of irregular tool wear on the change of cutting forces, the instrumented tool holder as a low-cost measuring device is used under the same process conditions to determine how sensitive the tool holder vibrations are to irregular edge wear. Within the instrumented tool holder, a single-axis MEMS-sensor (±100 g radial) with a vibratory mass is employed in a standard tool holder HSK-A 63 together with a telemetry system (Fig. 4). The adjustment of the accelerometer in the angular position is aligned to the active force component (± 5°). The acceleration signals are sampled at 9.5 kHz with 16 bit resolution.

3. Mechanical model of the measuring system

Although the frequency-dependent proportionality of force transients to acceleration can be found by means of machine dynamics, the model presented here is built on assumptions for milling applications. Thus, the following model for chipping determination represents a force approach for interpreting the data from a rotating and acceleration-sensitive sensor, which is implemented in the tool holder.

3.1. Kinematic and kinetic model

The tool holder is assumed to rotate with constant rotational speed ω_{Sp} around the z-axis. Within the instrumented tool holder,

Table 2
Analytical estimation of force due to tool geometry modification.

	Edge condition	γ in °	K_γ	h_{max} in μm	K_h	$h_{max} \bullet K_\gamma \bullet K_h$ in μm	Relative Force
Setup 1	C1.1 C1.2	−12 −12	1.18 1.18	107 131	1.46 1.41	184.6 218.4	100% 117%
Setup 2	C2 C1.2	−25 −12	1.31 1.18	95 143	1.49 1.39	185.7 234.9	101% 127%
Setup 3	C3 C1.2	−42 −12	1.48 1.18	76 162	1.55 1.36	174.3 260.5	94% 141%

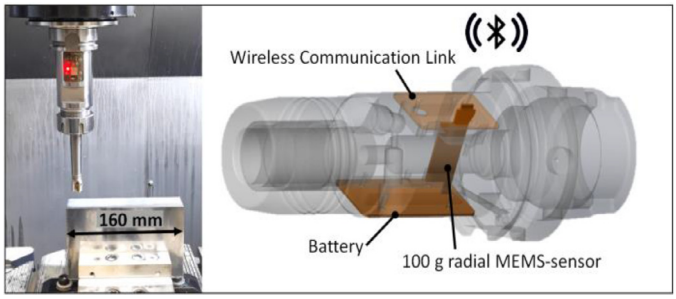

Fig. 4. Modified measurement setup with instrumented tool holder.

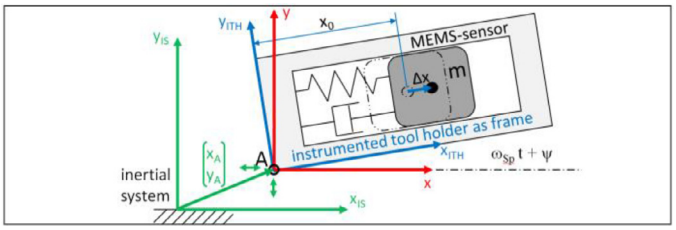

Fig. 5. Mechanical model for rotating MEMS-sensor.

the center of the vibratory mass m, which is incorporated in the MEMS-sensor shall be near the spindle axis A. In general, this axis and the center of gravity of the mass will never be exactly aligned or identical, because of the finite accuracy of assembly (static eccentricity x_0) and dynamical effects (additional eccentricity Δx), as depicted in Fig. 5.

The total acceleration of the mass m can be found using composite motion and relative kinematics. Making use of the tool holder's frame of reference, both the rotation and the time variant deflection of the holder (x_A, y_A) due to vibration need to be considered. A linear and frictionless spring-mass-damper-system is implemented. Applying Newton's second law leads to the differential equation of motion of the MEMS-sensor's mass.

$$\Delta\ddot{x} + \Delta\dot{x}\frac{c}{m} + \Delta x\left(\frac{k}{m} - \omega_{S_p}^2\right) = -\ddot{x}_A cos\left(\omega_{S_p} t + \psi\right) - \ddot{y}_A sin\left(\omega_{S_p} t + \psi\right) + x_0\omega_{S_p}^2 \quad (5)$$

Concerning the system's tuning and excitation, it can be concluded from the left-hand-side of Eq. (5) that the spindle rotation reduces the system's stiffness and misadjusts the sensor's tuning to a lower natural frequency. Furthermore, the sensor specifications in the data sheet correspond to its use in non-rotating systems. As a prerequisite, the sensor's natural frequency has to be much higher than the rotational speed.

The right-hand-side of Eq. (5) shows the effect of modulation due to rotation in x and y. Considering, that cutting forces cause an acceleration at A (x_A, y_A), only mixture products with trigonometric functions occur in the rotational sensor's excitation. This effect causes other frequencies to be detected in the instrumented tool holder than in stationary sensors. A constant offset in x and y due to eccentric assembly comes along with centripetal acceleration. In the frequency domain, the periodic directional dependency of A's acceleration, causing a mass movement, results in a nonlinear modulation. Both the multiplication with trigonometric functions in *x* and *y*, within the time domain, and theorems of Fourier-transformation enable the deduction of the modulation modes. According to theory, excitation-frequency Ω is measured as components in $\Omega \pm \omega_{Sp}$. The consideration of this effect is the basis for further interpretation of the data in the frequency domain.

3.2. Indicator for regularity

Based on the assumption of a non-rotating sensor and tools with regular pitch of number of teeth z ($z \geq 2$), cutting edge frequency-terms occur with $\Omega = z \bullet \omega_{Sp}$ and its k multiples. They are associated with the main cutting process and the regular creation of chips. Utilizing both, this hypothesis and the modulation scheme due to rotation, the instrumented tool holder's data power spectral density (*psd*), with knowledge of the nonlinear modulation, is evaluated around the frequencies of interest. This procedure aims to distinguish effects that emerge with every cutting edge from impacts that occur only once per rotation (like passing of a chipped edge). Summing up all effects caused by regular cutting and dividing this sum by the sum of all effects caused by periodical rotation, leads to a quotient *r*, hence, being a number from 0 to 1. In this context $r = 1$ refers to a fully regular milling operation, where all cutting edges cause almost identical vibrations. Eq. (6) describes the summation for the case of $z = 2$ cutting edges.

$$r(\Delta\omega, k) = \frac{\sum_{j=0}^{k} \int_{(2j+1)\omega_{Sp}-\Delta\omega}^{(2j+1)\omega_{Sp}-\Delta\omega} psd(\omega)d\omega}{\sum_{j=1}^{kx+1} \int_{j\omega_{Sp}-\Delta\omega}^{j\omega_{Sp}-\Delta\omega} psd(\omega)d\omega} \quad (6)$$

4. Acceleration signal analysis and classification

In order to evaluate the instrumented tool holder, 30 data sets within each set of tool conditions were determined by cutting tests. Tuning and combining of the postulated indicators for the presented setup were applied to find delimited signal areas with respect to the cutting edge conditions C1.1, C2, and C3. Thus, the classification problem for AI is evident, which implies in the developed algorithm, that less influence of the specific change of the cutting situation or detailed tool geometry but the mechanical regularity of the process is crucial.

Machine learning (ML) meets the needs of this problem. The indicator for regularity can be derived theoretically. However, it is not possible to predict which parameter set fits well. Statistical variance of the features, their combination and correlation can be evaluated. ML is able to compare and assess a large number of features of different types. All generated features rely on the mechanical model, predicting that a majority of the signal's power ought to be located within the areas around the expected frequency terms. 300 combinations of evaluation parameters (Table 3) are considered.

Each feature is a combination of three parameters, e.g. 1-0-9 (Fig. 6). Besides the window-function in time-domain, also two parameters for evaluating the spectra were changed and combined.

The maximum order of the tooth passing frequency describes the highest frequency terms considered for evaluation (in Fig. 6 up to the 5th order and its corresponding frequencies). Referring to this, the width around the observed frequency components (comb width) varied as well, from ±2.5% up to ±25% of the frequency. The same width is used for terms of regular cutting (numerator in Eq. (6)) and for those caused by spindle's rotation (denominator in Eq. (6)).

4.1. Feature comparison and correlation

Extra Trees Classifiers (ETC) [11], as an enhancement of the well-established Random Forest Method, is used to find the most indicative features and their combination for the set of measurement data. The basis of the method are decision trees. The random state of the generation of bootstrap data is varied to minimize wrong test settings. Multiple trees are randomly created, with the bootstrap data as input and get verified with the out-of-bag data. Different trees contain different amounts of features. Thus, there will be trees with less features achieving higher or the same accuracy than trees with more included features. By analyzing these trees, the performance of all features can be evaluated, the features get weighted and clarified as ranked. According to that ranking, the best and worst performing features are analyzed. It can be derived, that each window type is represented among the best features (see percentage distribution in Fig. 7a). The distribution of the 30 best performing features reveals

Table 3
Evaluation parameters.

Window parameter in time domain [first number]	Max. order of tooth passing frequency *k* [second number]		Comb width around the expected peaks $2 \bullet \Delta\omega$ [third number]	
Rectangle window [0]	5 [0]	25 [5]	0.05 [0]	0.30 [5]
	10 [1]	30 [6]	0.10 [1]	0.35 [6]
Hamming window [1]	15 [2]	35 [7]	0.15 [2]	0.40 [7]
	18 [3]	40 [8]	0.20 [3]	0.45 [8]
Hanning window [2]	20 [4]	42 [9]	0.25 [4]	0.50 [9]

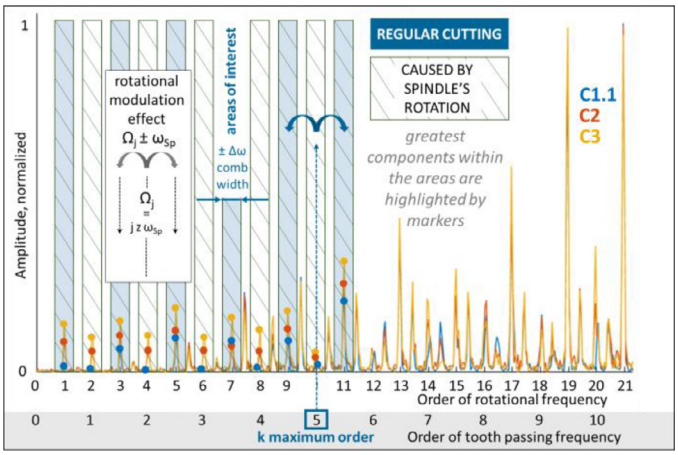

Fig. 6. Relation of amplitude spectrum for Feature 1-0-9.

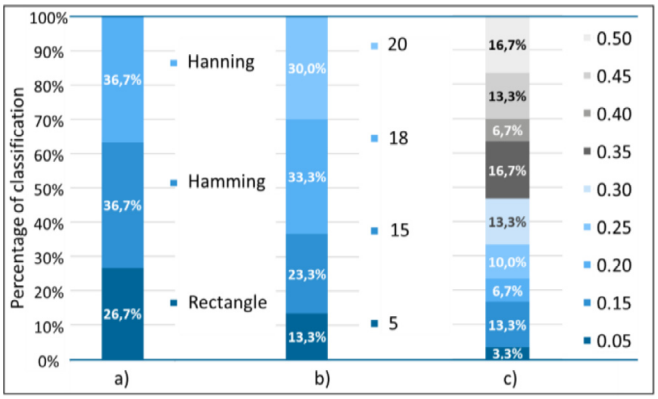

Fig. 7. Parameters distribution of 30 best features, a) window parameter in time domain, b) max. order of tooth passing frequency, c) comb width $2 \bullet \Delta\omega$.

that the maximum order of tooth passing frequency considered is 5, 15, 18 or 20, as Fig. 7b clearly shows. The comb width does not show any decisive difference (Fig. 7c). Furthermore, a similar analysis for the worst features can be acquired, which reveals that a rectangle window and a small comb width of 0.05 (Feature 0-x-0) are not suitable for detecting irregular tool wear like chipping or uneven tool wear.

In a standard ML-approach, a combination of several features is commonly used to classify data. Just taking the n-best features into consideration is not useful due to possible linear dependencies among the features. By detecting and plotting these correlations, a heatmap can be created. Both the correlation among the best features and the correlation among the worst features is very high. This can be explained by the finely tuned procedure, which defines 300 different, but similar features based on one theoretical model.

4.2. Feature utilization for process observation

Fig. 8 depicts the distribution of the highly ranked feature F1-4–6. It becomes evident, that a single, specifically designed and well-tuned indicator like F1-4–6 can be used to observe the occurrence of cutting edge chipping by the characteristics of the acceleration signal. However, in this particular case a simple threshold can be implemented to determine irregular tool wear.

By integrating this feature in a data analysis software, an in-process assessment of machining operations can be achieved. The use of an instrumented tool holder and acceleration measurement including a model-based signal analysis reveal required tool replacement. The

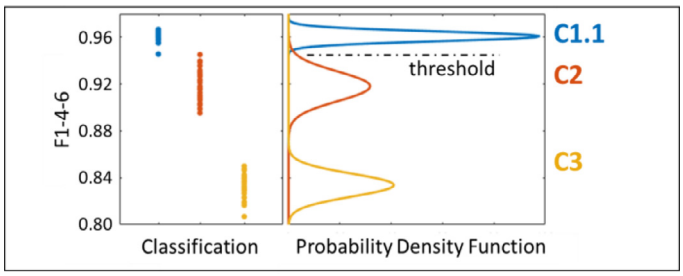

Fig. 8. Characteristic of F1-4–6 at different states of edge chipping.

clear separation of C1.1, C2, and C3 implies the possibility to find transitional states in between, thereby being more sensitive to uneven tool wear than shown in this study.

5. Conclusion

The prediction and thus the prevention of rapidly developing tool wear like edge chipping is a result of stochastic effects. An instrumented tool holder, a low-cost measurement system, can be used to evaluate acceleration signals close to the cutting zone. The regularity of the signals represents a criterion and measure for the wear state at single cutting edges of milling tools. A dynamic model of the MEMS sensor in the rotating coordinate system of the tool is used to compile the acceleration signals to different features, which are finally optimized by means of ML.

Using compact and fast algorithms to detect certain signal artefacts based on mechanical models, ML finds the most suitable parameter setting and finally enables in-process observation and even forecasting of the workpiece's quality.

Declaration of Competing Interest

The authors declare that they have no known competing financial interests or personal relationships that could have appeared to influence the work reported in this paper.

Acknowledgement

TU Wien as well as the authors want to express their appreciation and thanks to the Machine Tool Technologies Research Foundation (MTTRF) for supporting the research work.

References

[1] Bouzakis K-D, Michailidis N, Skordaris G, Bouzakisb E, Biermann D, M'Saoubi R (2012) Cutting with Coated Tools: Coating Technologies, Characterization Methods and Performance Optimization. *CIRP Annals* 61:703–723.
[2] Kumar M, Melkote S, M'Saoubi R (2012) Wear Behaviour of Coated Tools in Laser Assisted Micro-Milling of Hardened Steel. *Wear* 296:510–518.
[3] Neugebauer R, Denkena B, Wegener K (2007) Mechatronic Systems for Machine Tools. *Annals of the CIRP* 56/2:657–686.
[4] Möhring H-C, Nguyena QP, Kuhlmanna A, Lereza C, Nguyena LT, Mischa S (2016) Intelligent Tools for Predictive Process Control. *Procedia CIRP* 57:539–544.
[5] Brecher C, Wetzel A, Berners T, Epple A (2019) Increasing Productivity of Cutting Processes by Real-Time Compensation of Tool Deflection Due to Process Forces. *Journal of Machine Engineering* 19(1):16–27.
[6] Teti R, Jemielniak K, O'Donnell G, Dornfeld D (2010) Advanced Monitoring of Machining Operations. *CIRP Annals - Manufacturing Technology* 59(2):717–739.
[7] myTool IT GmbH, Weblink: www.ico-tronic.com/, Access: 20.01.2020
[8] Schörghofer P, Pauker F, Leder N, Mangler J, Ramsauer C, Bleicher F (2019) Using Sensory Tool Holder Data for Optimizing Production Processes. *Journal of Machine Engineering* 19(3):43–55.
[9] Denkena B, Biermann D (2014) Cutting Edge Geometries. *CIRP Annals - Manufacturing Technology* 63:631–653.
[10] Tschätsch H, Dietrich J (2008) Praxis der Zerspantechnik – Verfahren Werkzeuge Berechnungen, 9th Edition. *GVW Fachverlag Wiesbaden* .
[11] Pedregosa F, et al. (2011) Scikit-Learn: Machine Learning in Python. *Journal of Machine Learning Research* 12(2011):2825–2830.